Synthesis, characterisation and optimisation of bulk molecularly imprinted polymers from nonsteroidal anti-inflammatory drugs

S'busiso M. Nkosi[a,b*], Precious N. Mahlambi[c] and Luke Chimuka[d]

[a] *Department of Chemistry, Durban University of Technology, Durban, South Africa*
[b] *Technology Station in Chemicals, Mangosuthu University of Technology, uMlazi, South Africa*
[c] *School of Chemistry, University of KwaZulu-Natal, Scottsville, Pietermaritzburg, South Africa*
[d] *Molecular Sciences Institute, University of Witwatersrand, Johannesburg, South Africa*

Received 14 December 2020, revised 03 September 2021, accepted 03 September 2021

ABSTRACT

The scope of this study was to synthesise and characterise the multi-template molecularly imprinted polymer (MIP) and to use target compounds, naproxen, ibuprofen, diclofenac, fenoprofen and gemfibrozil as templates so as to achieve all maximum extraction efficiency for all compounds. These compounds are a class of nonsteroidal anti-inflammatory drugs (NSAIDs) generally used by humans, as they have pain-relieving activities. MIPs are cross-linked polymeric materials that display high binding capacity and selectivity towards templates of interest. The synthesis consisted of a bulk polymerisation process at 60 °C by using NSAIDs as multi-templates, ethylene glycol dimethacrylate (EGDMA), 2-vinyl pyridine (2VP) and toluene as cross-linker, functional monomer and porogen, respectively. Nonimprinted polymer (NIP) was synthesised in a similar manner with the omission of the templates. Characteristics of the polymers were analysed using Scanning Electron Microscopy (SEM), Fourier Transformed Infrared Spectroscopy (FTIR), Solid State Nuclear Magnetic Resonance Spectroscopy (NMR) and Thermal Gravimetric Analysis (TGA). An adsorption method of NSAIDs using the bulk polymerised MIP was investigated under various pH, mass, concentration and time conditions. Other parameters included adsorption kinetics and adsorption isotherms. Uptake of NSAIDs from an aqueous medium was achieved with 40 mg of MIP at pH 4.0 within 10 min of contact time. The extraction efficiencies achieved for NSAIDs in aqueous solutions ranged from 90–98% for all compounds tested. The adsorption capacity obtained for MIP ranged from 1.230–1.249 mg g^{-1} and 0.90–1.136 mg g^{-1} for NIP, whereas the selectivity values ranged from 1.12–2.4. A kinetic study revealed that adsorption obeys a second-order rate, and the Langmuir model explains adsorption isotherm data. This work showed that the multi-template approach for all the target compounds has the potential to give maximum extraction efficiencies in MIP extraction systems from aqueous samples.

KEYWORDS

bulk molecularly imprinted polymers, nonimprinted polymer, nonsteroidal anti-inflammatory drugs

INTRODUCTION

Numerous studies have disclosed that a number of pharmaceutical compounds are frequently detected in surface waters, making pharmaceuticals an increasing environmental concern for the last few years. [1-3] NSAIDs constitute one of the major groups of pharmaceuticals widely used globally. These pharmaceutical compounds are extensively employed for treating pains, fever and therefore represent the active constituent in many common painkillers.[4] Most studies have reported the occurrence of these pharmaceuticals in wastewater treatment plant (WWTP) influents due to human excretion.[5-8] Previous findings have reported that WWTPs are the major source of these substances in river water.[9] Also, some studies have indicated the existence of NSAIDs influent to sewage treatment plants (STPs),[10-13] just as in digested sludge with distinguished amounts in sludge mostly in the range of 10–100 ng g^{-1} dry weight.[14-15] One of the major concerns is that if such sludge is utilised for composting food crops, NSAID residues might be taken up into the plants and water, thus contaminating human and livestock food. The probable uptake of pharmaceuticals by plants from contaminated soil and water used for irrigation of crops has been widely reported.[16-19] Much of the time, pharmaceuticals are taken by roots and moved into different tissues by transpiration and diffusion. Because of the plant uptake, these substances in food sources, for example, vegetables, are a public concern.[20-23]

Molecular imprinting is a method used to synthesise polymers with highly specific binding sites for tiny particles.[24] These polymers are prepared using a functional monomer(s), which permits the interactions with the functional group(s) of a template to be recognised, and they are prepared with a cross-linking monomer(s) in the presence of the target molecule(s). The imprint molecule(s) is detached from the polymer to create the molecularly imprinted complementary binding site(s) for the target molecule(s).[25] In the course of the most recent twenty years, MIPs have gained frequent scientific applications that incorporate their utilisation as; solid-phase extraction (SPE) sorbents,[26] chromatographic stationary phase,[27-29] and electrochemical sensor.[30] The popularity of MIPs in science applications is ascribed to their properties that include high selectivity, mechanical strength, and resistance against acids, bases, organic solvents, high pressures and temperatures.[31-33] Much work has been coordinated towards using MIP to extract a single compound from different aqueous samples.[34-36] However, little research has been done on aqueous solutions using multi-templates MIP, especially on NSAIDs. A study on synthesis, characterisation and optimisation of magnetite MIPs for the application in the removal of NSAIDs was reported by Mamman et al.[37] In separate studies by Madikizela et al., the determination of ibuprofen, naproxen, and diclofenac in aqueous samples was reported using a multi-template MIP as a selective adsorbent for solid-phase extraction.[38] Elsewhere, selective removal of acidic pharmaceuticals from contaminated lake water using multi-templates MIP was reported by Dai et al.[39] Given the scope presented above, a novel MIP was prepared via template-directed molecular imprinting by a non-covalent imprinting scheme. The materialisation of a number of pharmaceutical molecules imprinted in the polymer matrix was investigated using an NSAIDs mixture standard consisting of five pharmaceuticals, naproxen, ibuprofen, diclofenac, fenoprofen,

*To whom correspondence should be addressed
Email: nkosis@mut.ac.za

ISSN 1996-840X Online / South African Chemical Institute / http://saci.co.za/journal

https://doi.org/10.17159/0379-4350/2022/v76a09

and gemfibrozil (Figure 1). A functional monomer is known to be a compound that is responsible for the binding interactions in the imprinted binding sites. In a non-covalent imprinting approach, a functional monomer is used in excess relative to moles of a template to favour the formation of template-functional monomer assemblies. In the current study, 2-vinyl pyridine was selected as the functional monomer. This monomer can form hydrogen bonds with the target molecules' carboxylic group, as shown in the scheme (Figure 2). The optimisation of the resulting polymer, including adsorption properties, isotherms, kinetics and selectivity, were discussed, and the effect of pH, contact time and MIP amount on extraction efficiencies were also investigated. The physical properties of the template molecules are shown in Table 1.

EXPERIMENTAL

Reagents

Gemfibrozil (98%), Ibuprofen (≥98%), Fenoprofen ((≥98%), Naproxen (98%), Diclofenac sodium salt, 2-vinyl pyridine (97%), Ethylene glycol dimethacrylate (98%), 1,1′-azobis-(cyclohexanecarbonitrile) (98%), high performance liquid chromatography (HPLC) grade acetone (≥99.8%), HPLC grade methanol (≥99.8%) and toluene (99.7%) were purchased from Sigma-Aldrich (Steinheim, Germany). The structure of the target pharmaceuticals is shown in Figure 1. HPLC-grade acetonitrile (≥99.9%) and glacial acetic acid (100%) were purchased from Merck (Darmstadt, Germany). Formic acid (approx. 98%) was purchased from Fluka (Steinheim, Germany).

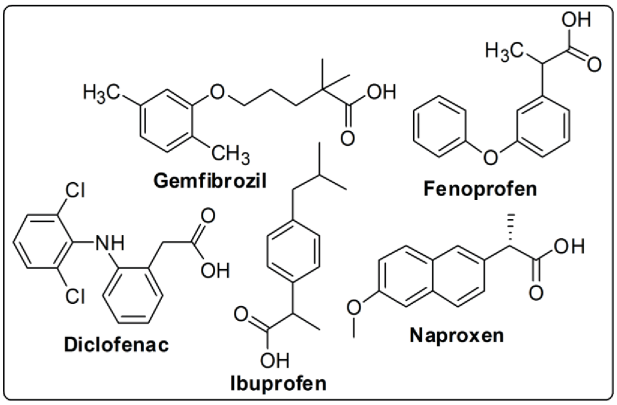

Figure 1: Molecular structures of the template molecules

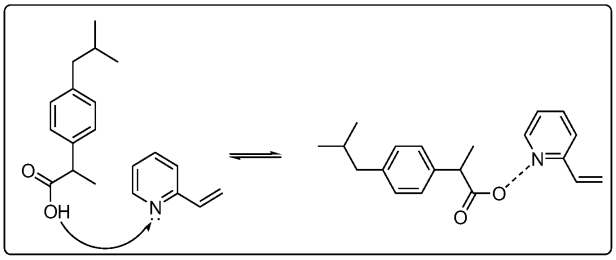

Figure 2: Templates interactions with the functional monomer

Table 1: Physical properties of the template molecules

Compound	Formula	Molecular weight	pK_{ab}	Water solubility	Log k_{ow}
Diclofenac	$C_{14}H_{11}Cl_2NO_2$	296.2	4.0	4.52	4.5
Gemfibrozil	$C_{15}H_{22}O_3$	250.3	4.7	8.42	4.8
Ibuprofen	$C_{13}H_{18}O_2$	206.3	4.4	41.1	4.0
Naproxen	$C_{11}H_{14}O_3$	230.3	4.2	44.1	3.2
Fenoprofen	$C_{15}H_{14}O_3$	242.3	4.5	30.0	4.0

Instrumentation

Chromatographic separation was performed on an HPLC system with an online mobile phase degasser unit (Model: DGU-20A3), UV/vis detector (Model: SPD-20A), 20 µL sample loop and pump (Model: LC-20AB), all obtained from Shimadzu Corporation (Kyoto, Japan). The mobile phase comprised of a mixture of acetonitrile: 0.2% formic acid in water (70:30, v:v) at a flow rate of 0.8 mL min^{-1}. Separation was performed on a Kinetex C18 HPLC column of 150 × 4.6 mm × 2.6 µm attained from Phenominex (California, USA). For data collection and processing, Shimadzu LC solutions software was used. The UV/vis detector was set at 230 nm and 200 nm for all template measurements. The FTIR characterisation was recorded using a 1600 Paragon Spectrophotometer from PerkinElmer. TGA was performed using a TA instrument, model SDTQ600. TGA curves were recorded at a heating rate of 10 °C min^{-1} from 30 °C to 700 °C under a nitrogen purge of 50 mL min^{-1}. SEM, Zeiss Merlin Field Emission Scanning Electron Microscope (FESEM), electron image EHT (kV) probe, was used to study the polymer morphology. The solid-state ^{13}C CP/MAS NMR was performed by Varian VNMRS 600 MHz NMR. The spectra were obtained utilising a dual-channel 4 mm che-magnetics probe using 4 mm zirconia rotors. The cross-polarisation (CP) spectra were recorded at 25 °C with proton decoupling using a recycle delay of 10s. The CP pulse power parameters were optimised for the Hartmann-Hahn match using a glycine standard sample. The contact time for cross-polarisation was optimised to 2.0 ms. Magic-angle-spinning (MAS) was performed at 10 000 revolutions per second (10 kHz).

Synthesis of polymers

A procedure reported by Madikizela et al. [40] was applied with alteration for the synthesis and bulk polymerisation of a polymer in two stages reaction process. The first step was carried out by dissolving all the templates, ibuprofen (0.1 mmol), naproxen (0.1 mmol), diclofenac (0.1 mmol), fenoprofen (0.1 mmol) and gemfibrozil (0.1 mmol) and 54 µL 2-vinyl pyridine (2-VP) and a mixture of acetonitrile/toluene (1:3, v:v). The mixture was stirred in a 250 mL round bottom flask for 30 minutes at room temperature. In the second step, 4.77 µL EGDMA was added along with 100 mg 1,1′-azobis-(cyclohexanecarbonitrile), used as a radical initiator. The mixture was purged with nitrogen gas for 10 minutes, sealed and stirred in an oil bath at 60 °C for 16 hours to initiate polymerisation. After 16 hours, the temperature was increased to 80 °C and maintained for 24 hours to achieve a solid polymer. The resulting polymer was oven-dried at 80 °C to constant mass. NIP was prepared under the same conditions in the absence of the template molecules.

Removal of the template

The removal of the imprinting templates to free the imprinted cavities was performed using the dry MIP by the Soxhlet extraction technique. A mixture of 10% (v/v) acetic acid in methanol was used to elute the templates from the polymer. The elution step was repeated multiple times until the HPLC system no longer detected the templates. Subsequently, 100% acetonitrile was used to wash off the acetic acid.

Grinding and sieving of the polymers

The polymer was milled, sieved and particles ranging from 25 to 50 µm were collected. For the entirety of the subsequent analysis, the particle size portion used was 25 µm, and the fraction above 50 µm was used for characterisation.

Batch adsorption and optimisation studies

The adsorption experiments for both polymers were evaluated at ambient temperature using deionised water previously spiked with 5 mg L^{-1} naproxen, ibuprofen, diclofenac, fenoprofen and gemfibrozil.

These experiments were done to study the effect of pH (2.5–10), MIP mass (10–50 mg) and adsorption time (10–60 min) on extraction efficiency. Just one parameter at a time was changed while the others were kept constant during the optimisation. The effect of the adsorption medium was also investigated using acetone, acetonitrile, toluene, methanol and water. Initially, a 10 mL solution containing NSAIDs standard (5 mg L^{-1}) was prepared in each solvent, and the adsorption process was allowed to occur at optimum MIP amount and optimum contact time. It was important to consider this process as it has been reported that the type of solvent used to dissolve the target compound is known to impact the batch adsorption capacity for the MIP.[41] The NSAIDs standard prepared in water was treated likewise. Extraction efficiency was determined for each situation. Each experiment was conducted in triplicates. The extraction efficiency, the quantity of each NSAID extracted by MIP, was determined as the variance between the spiking amount and the residual amount in solution after extraction using equation (1). The adsorption capacity, the maximum amount of each NSAID adsorbed by a unit mass of MIP, was determined using equation (2), where C_0 symbolises the initial concentration (mg L^{-1}) before the adsorption and C_e the final concentration (mg L^{-1}) of target compound remaining in solution after adsorption. V is the volume (L) of the solution, and W represents the mass of the polymer in grams. [42-43]

$$\text{Extraction efficiency}(\%) = \frac{(C_o - C_e)}{C_o} \times 100 \quad (1)$$

$$\text{Adsorption capacity}\left(\text{mg. g}^{-1}\right) = \frac{(C_o - C_e)}{W} V \quad (2)$$

The adsorption procedure was explained using equation (3) and equation (4) for pseudo-first-order and pseudo-second-order kinetic models. The adsorption mechanism was explained using the model with the higher R^2 value, where Q_e and Q_t are adsorption capacity parameters (mg g^{-1}) at equilibrium and at a time, t (min), respectively. K_1 and K_2 are Lagergren pseudo-first-order (min^{-1}) and pseudo-second-order sorption rate constants, respectively.[44–45]

$$\log(Q_e - Q_t) = \log Q_e - \frac{K_1 t}{2.303} \quad (3)$$

$$\frac{t}{Q_e} = \frac{1}{K_2 Q_{e^2}} + \frac{t}{Q_e} \quad (4)$$

The extent of adsorption and the isothermal analysis of the polymers were explained using equations (5) and (6) for the linearised form of Freundlich and Langmuir isotherms, respectively. Where m is the adsorption intensity or surface heterogeneity, C_e is the adsorption capacity of the target molecule (mg g^{-1}), Q_{max} is the maximum adsorption capacity (mg g^{-1}), and K_L is the Langmuir adsorption equilibrium constant.[46] The constants K_L and Q_{max} were determined using the intercepts and slopes of the linear plots of C_e/Q versus C_e.

$$\log Q = m \log C_e + \log \alpha \quad (5)$$

$$\frac{C_e}{Q} = \frac{C_e}{Q_{max}} + \frac{1}{Q_{max K_L}} \quad (6)$$

Selectivity study

The selectivity of the MIP for NSAIDs was conducted at room temperature in batch rebinding experiments using optimum conditions, which were deionised water (pH 4.0) that was previously spiked with 5 mg L^{-1} mixture of gemfibrozil, diclofenac ibuprofen, naproxen, fenoprofen and ketoprofen (as a competitor). The spiked solution (10 mL) was poured into a flask containing 40 mg of the MIP. The resulting solution was stirred at ambient temperature for 10 minutes and transferred into 3-mL SPE tubes. Frits were placed below and above the MIP to avoid losing sorbent, and liquid fractions were sent to waste. After that, the concentration of the un-adsorbed compounds in the solution was quantified with HPLC. The competitive adsorption of NSAIDs from their mixtures in the presence of ketoprofen was then conducted. The effect of imprinting on selectivity was calculated using equation (7). Where K_d (mg g^{-1}) is the distribution coefficient, C_0 is the initial solution concentration, C_e is the final solution concentration, V (mL) is the volume of the solution, and W (mg) is the weight of the polymer. Furthermore, the selectivity coefficient for the binding of NSAIDs compounds in the existence of a competitor was calculated regarding equation (8), where K is the selectivity coefficient. Also, the selectivity of the MIP with respect to the NIP was obtained using the relative selectivity coefficient (K') according to equation (9).

$$K_d = \frac{C_o - C}{W} V \quad (7)$$

$$K = \frac{K_d(\text{Template})}{K_d(\text{Competitor})} \quad (8)$$

$$K' = \frac{K_{MIP}}{K_{NIP}} \quad (9)$$

RESULTS AND DISCUSSION

Synthesis and characterisation

The FTIR spectra for polymers (Figure 3) are more or less comparable to one another, consistent with the fact that both polymers were prepared based on the same monomer, cross-linker and initiator. All the significant peaks agreed with the information acquired from previous studies.[46, 47] The interface between templates and monomer offered changeable peaks in the spectrums, which exhibited a broad OH stretching vibration peak at 3500 cm^{-1} for MIPs. These peaks can be related to the methacrylic acid carboxylic group (COOH). The -CH_2 stretching peak was likewise seen at 2900 cm^{-1} due to the methylene group in 2-VP and EGDMA. The carbonyl group C=O stretching peak was seen in both MIP and NIP at 1700 cm^{-1}, which might have originated from the template and cross-linking molecules. Weak arrangement bands from 1600 cm^{-1} to 1200 cm^{-1} and sharp bands at 1100 cm^{-1} specifically on MIPs spectra demonstrate the presence of an aromatic ring of the target compounds.

SEM was used to analyse the surface morphology and the particle size for both MIP and NIP. The results (Figure 4A and B) indicate that the type of particles obtained was all found to be more irregular for both polymers. The control polymer (NIP) was seen to have a smoother surface than the MIP. In contrast, the MIP, after the removal of the template on the opposite side, had rough surfaces. These rough surfaces can be ascribed to the development of cavities during the synthesis method. A previous study has documented that the roughness of MIP particles can prompt high surface area than that of

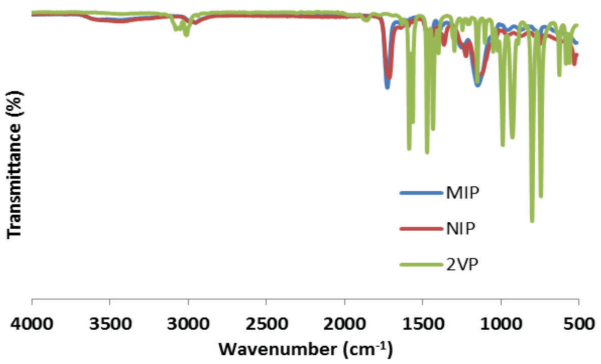

Figure 3: FTIR spectra for MIP, NIP and monomer

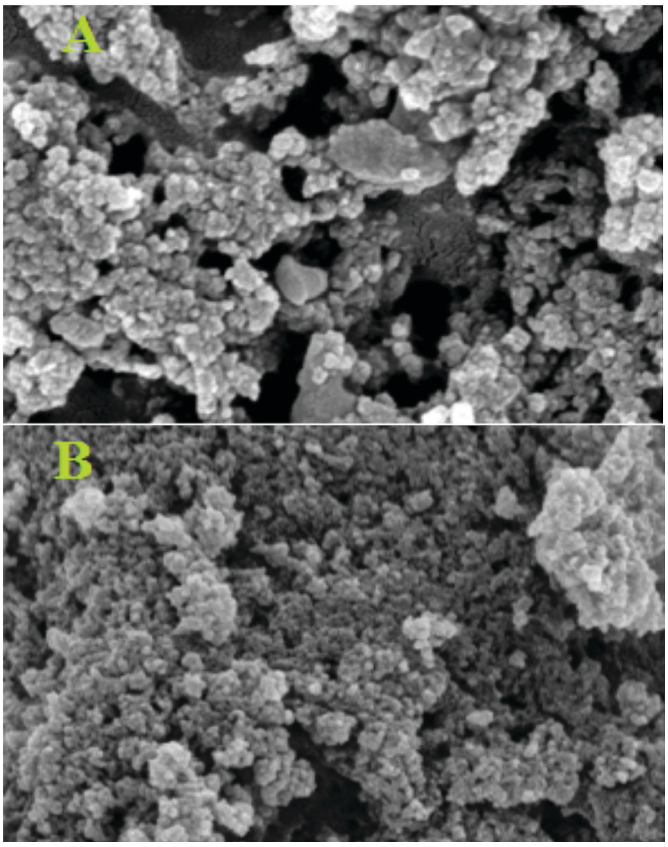

Figure 4: SEM micrographs of A = MIP and B = NIP

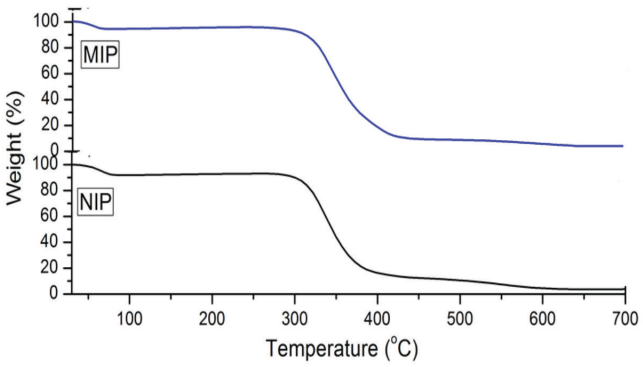

Figure 5: Thermogravimetric analysis of the synthesised MIP and NIP

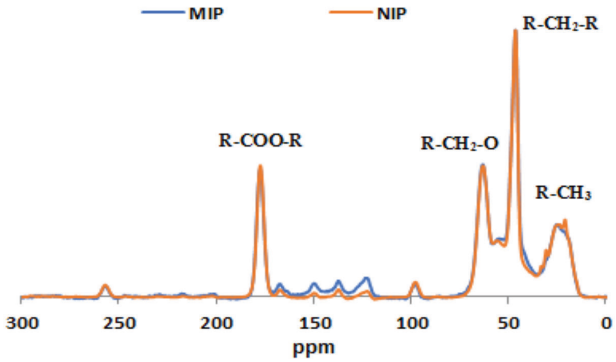

Figure 6: Solid-state ^{13}C CP/MAS NMR Spectra of MIP and NIP

the control polymer. Thus MIP can adsorb analytes of interest superior to the control polymer.[48]

TGA was performed to investigate thermal stability for both MIP and NIP (Figure 5). At 50 °C, MIP and NIP had a mass loss of around 5% and 7%, respectively. Thermal decomposition of polymers was further observed at 280 °C, which was noticeable as the temperature where the polymer spine collapses. In literature, the polymer spine collapsed at 300 °C for MIP synthesised for 2-phenyl propionic acid NSAIDs.[49] The polymers then attain total decomposition from 400 °C. The difference may have been brought about by structural variations that might have occurred during the removal of the template procedure.

The solid-state ^{13}C CP/MAS spectra for the MIP and NIP (Figure 6) were performed by NMR. In comparing the spectra for both polymers, there are no dissimilarities in the chemical shifts or comparative signal intensities observed, which indicates that the materials were chemically equivalent. All signals could be allocated in agreement with the anticipated arrangement of the polymers, and the relevant peaks were in agreement with the data obtained from previous studies.[50–51] The resonances illustrated that correspond to the several methyl groups were represented by the broad peak at 23 ppm. Other groups identified were methylene groups in cross-linker at 47 and 65 ppm and the CO_2R group at 175 ppm. These results were expected, given the type and the nature of imprinting, which uses a large amount of EGDMA and 2-VP. At the same time, carbonyl grouping in CO_2R is distinctly observable at the far end, which agrees with the literature results.[50, 52]

Optimisation of adsorption studies

The monomer-template interaction was promoted by adjusting the pH of the water solutions. The pH was investigated in the range (2.5–10). The study showed that pH 4 was optimum as polymers could adsorb the target compounds. They demonstrated that maximum adsorption efficiency decreases with increased pH (Figures 7 and 8). This pH increase might be attributed to the hydroxide ions interferences in MIP cavities. The same trend was observed with other studies in the

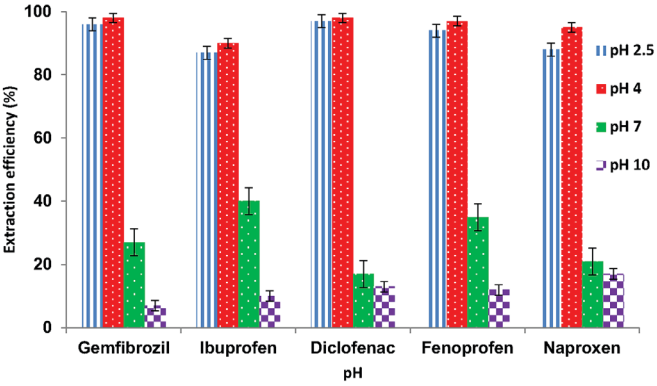

Figure 7: Effect of pH on MIP extraction efficiency

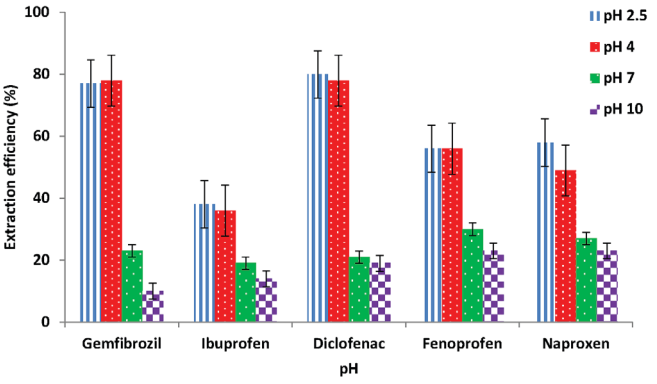

Figure 8: Effect of pH on NIP extraction efficiency

literature.[40, 53] It was also noted that the adsorption efficiency decreases with the decrease in pH below 4. This adsorption efficiency decrease can be due to an easy protonation of the monomer via the lone pair

making it rebinding problematic. Therefore, pH 4 was chosen as an ideal and used in all succeeding experiments. The effect of pH is essential to accomplish maximum extraction of target compounds. For the adsorption of acidic pharmaceuticals, it has been documented that the extraction depends on the hydrogen bonding of the targeted compounds and functional monomer.[54]

Batch adsorption was carried out by varying the amount of MIP from 10 to 50 mg, while parameters such as the sample pH (4.0), concentration of the target compounds (5 mg L^{-1}), sample volume (10 mL) were constant. Results in Figure 8 indicated that when 40 mg of the MIP was employed, the extraction efficiencies ranged from 95–98% for all the tested compounds. The closeness of the range of extraction efficiencies could be due to the use of multi templates, indicating that all target compounds had pretty much equivalent possibility of getting adsorbed. It was seen that higher extraction efficiencies were obtained for the MIP (Figure 9) compared to NIP (Figure 10). This difference in extraction efficiencies maybe because of the polymer imprinting effect. Hence, adsorption experiments were subsequently carried out using 40 mg of the polymer.

While the sample pH (4.0), initial concentration (5 mg L^{-1}), adsorbent mass (40 mg) and sample volume (10 mL) were kept constant, the effect of contact time (Figure 11) was studied by determining the extraction efficiency as a function of time. The extraction efficiencies more prominent than 70% were attained within 10 minutes of contact time between NSAIDs and adsorbents (Figure 10). In order to ensure the regularity uptake of target compounds from aqueous samples, the contact time of 10 min was employed in subsequent experiments. In a previous study,[40] the results obtained revealed that when 50 mg of the MIP was used, more than 91% of ibuprofen and naproxen were extracted, diclofenac extraction efficiency was achieved at 100%. Higher extraction efficiencies were obtained for the MIP than the NIP. NSAIDs were observed to have an expressive improvement in extraction efficiencies, especially naproxen after 10 min, indicating that MIP had more binding sites conformation on its surface for NSAIDs adsorption, likely because of removal of templates. The same could not be said with NIP (Figure 12) as it reached its saturation point within 20 min. MIP adsorption capacity ranged from 1.229–1.249 mg g^{-1} and from 0.901–1.125 mg g^{-1} for NIP, as shown in Table 2. These were comparable with adsorption capacities studied by Santosda, where adsorption capacities for MIPs ranged from 0.35–1.82 mg g^{-1}, for the study on the assessment of surfactants on the performance of MIPs toward adsorption of pharmaceuticals.[55]

The uptake of compounds from different solvent conditions was evaluated, and the solvents were studied in the increasing polarity order; water, acetonitrile, methanol, acetone and toluene. The effect of the adsorption medium indicates that the highest extraction efficiency (>90%) was achieved when NSAIDs were dissolved in toluene (Figure 13). The results were somewhat anticipated as the porogenic solvent used in this study was toluene and is least polar. This solvent has little effect that disrupts monomer and template binding interactions. Good extraction efficiencies (>80%) were obtained for all compounds in water, acetonitrile, methanol, acetone and toluene, except for diclofenac.

Kinetic modelling

The rate of the adsorption of the NSAIDs by MIP and NIP was measured as a function of time. If second-order kinetics is applicable, the plot of t/Q versus t is expected to give a straight line. The values K_2 and Q_e were calculated from the intercept and the plot slope, respectively; the data is presented in Table 3.

Table 2: Adsorption capacity on contact time

Compound	MIP	NIP
Diclofenac	1.247	1.112
Gemfibrozil	1.249	1.112
Ibuprofen	1.246	1.123
Naproxen	1.232	1.125
Fenoprofen	1.229	0.901

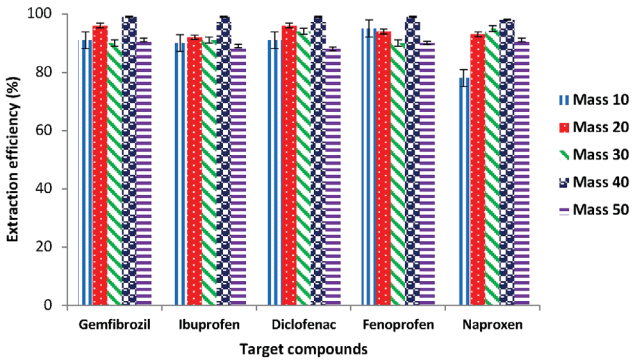

Figure 9: Effect of MIP amount on extraction efficiency

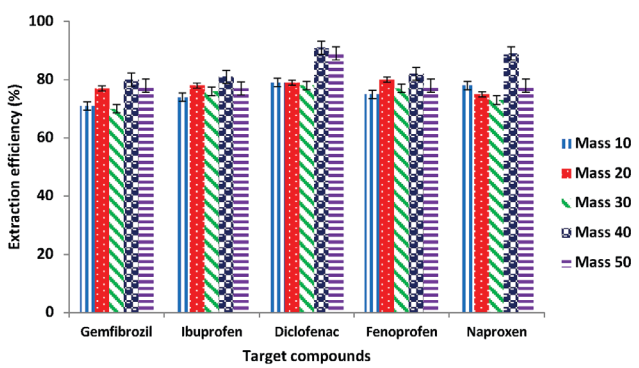

Figure 10: Effect of MIP amount on extraction efficiency

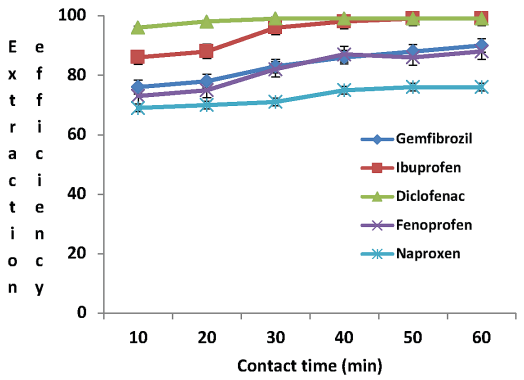

Figure 11: Effect of MIP contact time on extraction

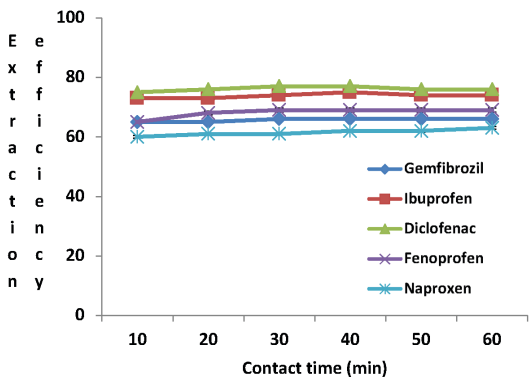

Figure 12: Effect of NIP contact time on extraction

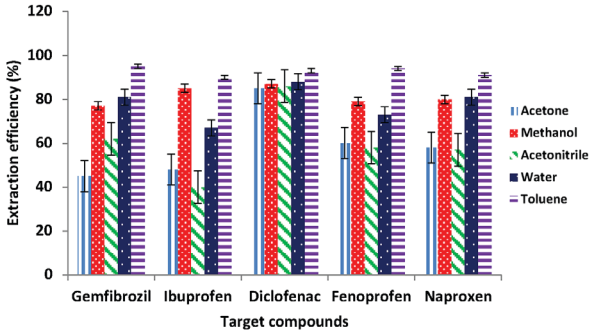

Figure 13: Effect MIP porogenic solvent on extraction efficiency

Table 3.: Calculated data for the kinetic models

Polymer	Compound	Pseudo-first-order	Pseudo-second-order		
		R^2	R^2	K_2 (g mg^{-1} min^{-1})	Q_e (mg g^{-1})
MIP	Gemfibrozil	0.8256	0.9998	10.1	1.230
	Fenoprofen	0.8888	0.9999	4.01	1.117
	Naproxen	0.8532	0.9997	3.50	1.236
	Diclofenac	0.3252	0.9990	11.8	1.411
	Ibuprofen	0.9423	0.9960	12.1	1.350
NIP	Gemfibrozil	0.8365	0.9982	0.92	0.930
	Fenoprofen	0.8979	0.9822	3.58	0.850
	Naproxen	0.7510	0.9950	2.91	1.128
	Diclofenac	0.6325	0.9238	3.75	1.096
	Ibuprofen	0.9216	0.9888	0.09	1.255

The kinetic modelling results showed that the adsorption process follows pseudo-second-order kinetics. A pseudo-first-order model did not obey the straight line; a low correlation coefficient (R^2) value of 0.9423 compared to 0.9999 for the pseudo-second-order model was obtained, indicating the first-order kinetic model is less appropriate. The pseudo-second-order equation gradient was used to estimate the adsorption capacities. The adsorption capacities obtained for MIP were 1.230, 1.117, 1.236, 1.411 and 1.350 mg g^{-1} for gemfibrozil fenoprofen, naproxen, diclofenac and ibuprofen, respectively. The maximum adsorption capacities from the batch adsorption experiments were 1,249, 1,248, 1.238, 1.247 and 1.248 mg g^{-1} for gemfibrozil, fenoprofen, naproxen, diclofenac and ibuprofen, respectively. The experimental adsorption capacities were within the standard deviation of the calculated values, suggesting there was a good agreement between the two processes. The pseudo-second-order kinetic results and the Langmuir adsorption isotherm modelling results can be acknowledged and accepted in describing the magnitude of adsorption on NSAIDs in MIP cavities.

Adsorption isotherms

The amount of materials adsorbed is determined as a function of the concentration at a constant temperature that could be explained in adsorption isotherms. Adsorption isotherms were investigated for NSAIDs with MIP and NIP using the optimised conditions. Langmuir and Freundlich established equations utilised to portray the experimental isotherm information. The Langmuir model is considered the most popular and widely applied adsorption isotherm.[56–57] The adsorption data were analysed using the linear form of the Langmuir isotherm. The Freundlich expression is an exponential equation and therefore presumes that the sorbate concentration on the adsorbent surface increases as the increase of sorbate concentration. The applicability of the Freundlich sorption was additionally examined by plotting log Q_e versus log C_e. The constant K_L and Q_{max} were determined using the intercepts and slopes of the linear plots of C_e/Q versus C_e. Given the correlation coefficients acquired, the information fitted well with the Langmuir isotherm. Therefore, the solid match and good fit for Langmuir isotherm was possibly proof of the overwhelming status of the compound adsorption, which may frequently prompt monolayer adsorption on the surface of the adsorbents. Table 4 shows data extracted from the adsorption isotherms. As expected, the obtained maximum adsorption capacities for the MIP were higher than those for NIP; since MIP has more binding sites than the NIP.

Selectivity studies

The selectivity of the MIP was assessed using equations (7–9) described earlier. During the experiment, deionised water was spiked with 5 mg L^{-1} of target compounds in the presence of equal amounts of ketoprofen is used as a competitor in a multi-component process. Ketoprofen is an acidic pharmaceutical with more or less similar physicochemical properties and size as the target compounds. It extensively coexists with all the mentioned targets in water bodies. It was expected that these compounds would form hydrogen bonds with 2-VP, which was used as a monomer during imprinting due to the presence of the carboxylic group in these compounds' chemical structure. The HPLC separation of ketoprofen from other compounds was achieved using the conditions in section 2.2. Also, K′ values of the imprinted polymers were compared with ketoprofen to estimate the influence of imprinting on selectivity. The binding capacities of the compounds on MIP were higher than NIP. Table 5 summarises the KD, K and K′ valuesof the compounds. The K′ values for diclofenac, gemfibrozil, fenoprofen, naproxen and ibuprofen were 1.12, 2.4, 1.38, 1.55 and 1.28, respectively. The selectivity of MIP and NIP towards NSAIDs in the presence of ketoprofen revealed that MIP has a greater selectivity towards the target compounds than NIP in aqueous samples (Figure 14). Elsewhere, [39] the results showed that MIP also displayed high adsorption efficiencies for

Table 4: Data extracted from the adsorption isotherms

Polymer	Compound	Langmuir			Freundlich
		R^2	K_1 (L mg^{-1})	Q_{max} (mg g^{-1})	R^2
MIP	Gemfibrozil	0.9146	1.568	4.897	0.6998
	Fenoprofen	0.9193	0.356	3.655	0.8343
	Naproxen	0.9999	0.328	4.852	0.8950
	Diclofenac	0.9999	1.160	5.643	0.9918
	Ibuprofen	0.4681	0.746	3.388	0.9171
NIP	Gemfibrozil	0.8565	2.666	4.223	0.9082
	Fenoprofen	0.9179	0.879	3.111	0.9822
	Naproxen	0.9721	0.268	3.783	0.8835
	Diclofenac	0.9930	2.139	4.719	0.9238
	Ibuprofen	0.9922	0.792	3.044	0.9555

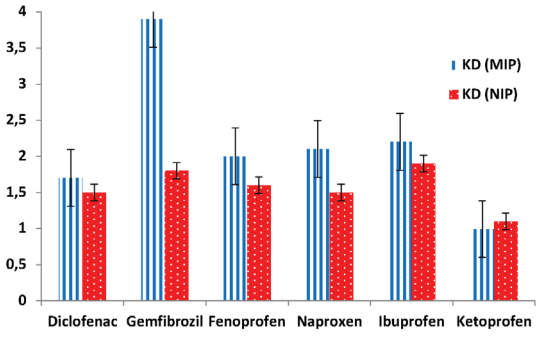

Figure 14: Selectivity study of templates in the presence of competitor

Table 5: Selectivity data of templates in the presence of competitor

Templates	K_D(MIP) (mg g^{-1})	K_D (NIP) (mg g^{-1})	K (MIP)	K (NIP)	K′
Diclofenac	1.7	1.5	1.52	1.36	1.12
Gemfibrozil	3.9	1.8	3.94	1.64	2.40
Fenoprofen	2.0	1.6	2.00	1.45	1.38
Naproxen	2.1	1.5	2.12	1.36	1.55
Ibuprofen	2.2	1.9	2.22	1.73	1.28
Ketoprofen	1.0	1.1	–	–	–

five targeted compounds in the presence of two competitors. The K_D values on the selectivity of MIP followed the order of gemfibrozil > ibuprofen > naproxen > fenoprofen > diclofenac, which could suggest that the imprinting cavities of the compounds were created based on the interaction of shape, size, and amount of hydrogen bonding and functionality of the template. Even in multi-template MIPs, some compounds are more preferred than others.

CONCLUSION

A novel multi-template MIP was successfully synthesised by the bulk polymerisation process. FTIR confirmed that both polymers have a similar backbone structure. TGA results revealed that both MIP and NIP have similar backbone structures, with slight differences which might have been caused by structural variations that might have materialised during the template removal process. In comparing the NMR spectra for MIP and NIP, no differences were observed in the chemical shifts or relative signal intensities, implying that the materials were chemically alike. SEM results showed that the surface of the MIP was more irregular and rougher than NIP. The adsorption of target compounds by MIP was viable at pH 4.0. Higher extraction efficiencies for all target compounds were achieved using MIP than NIP due to the advantageous use of multi-templates. The adsorption kinetics was best fitted with pseudo-second-order, which indicates that chemisorption occurred. Although similarities were noticed for both MIP and NIP in polymer characterisation results, experiments on selectivity for MIP demonstrated a high selectivity towards gemfibrozil than other compounds.

ACKNOWLEDGEMENTS

Technology Innovation Agency financially supported this study through its core grant to the Technology Station in Chemicals of Mangosuthu University of Technology (no core grant number provided). Special thanks to the Durban University of Technology's HPLC laboratory co-workers.

ORCID iDs

S'busiso Nkosi – https://orcid.org/0000-0002-8257-2592
Precious Mahlambi – https://orcid.org/0000-0003-0179-7165
Luke Chimika – https://orcid.org/0000-0002-8552-2478

REFERENCES

1. Kümmerer K, editor. Pharmaceuticals in the Environment. 2nd ed. Berlin: Springer-Verlag; 2004. https://doi.org/10.1007/978-3-662-09259-0.
2. Halling-Sørensen B, Nors Nielsen S, Lanzky PF, Ingerslev F, Holten Lützhøft HC, Jørgensen SE. Occurrence, fate and effects of pharmaceutical substances in the environment—a review. Chemosphere. 1998;36(2):357–393. https://doi.org/10.1016/S0045-6535(97)00354-8.
3. Farrington K, Regan F. Investigation of the nature of MIP recognition: the development and characterisation of a MIP for Ibuprofen. Biosens Bioelectron. 2007;22(6):1138–1146. https://doi.org/10.1016/j.bios.2006.06.025.
4. Larsson E, Al-Hamimi S, Jönsson JA. Behaviour of nonsteroidal anti-inflammatory drugs and eight of their metabolites during wastewater treatment studied by hollow fibre liquid phase microextraction and liquid chromatography mass spectrometry. Sci Total Environ. 2014;485/486:300–308. https://doi.org/10.1016/j.scitotenv.2014.03.055.
5. Dahane S, Gil García MD, Martínez Bueno MJ, Uclés Moreno A, Martínez Galera M, Derdour A. Determination of drugs in river and wastewaters using solid-phase extraction by packed multi-walled carbon nanotubes and liquid chromatography-quadrupole-linear ion trap-mass spectrometry. J Chromatogr A. 2013;1297:17–28. https://doi.org/10.1016/j.chroma.2013.05.002.
6. Migowska N, Caban M, Stepnowski P, Kumirska J. Simultaneous analysis of non-steroidal anti-inflammatory drugs and estrogenic hormones in water and wastewater samples using gas chromatography-mass spectrometry and gas chromatography with electron capture detection. Sci Total Environ. 2012;441:77–88. https://doi.org/10.1016/j.scitotenv.2012.09.043.
7. Martín J, Camacho-Muñoz D, Santos JL, Aparicio I, Alonso E. Occurrence of pharmaceutical compounds in wastewater and sludge from wastewater treatment plants: removal and ecotoxicological impact of wastewater discharges and sludge disposal. J Hazard Mater. 2012 Nov 15;239/240:40–47. https://doi.org/10.1016/j.jhazmat.2012.04.068.
8. González-Barreiro C, Lores M, Casais MC, Cela R. Simultaneous determination of neutral and acidic pharmaceuticals in wastewater by high-performance liquid chromatography-post-column photochemically induced fluorimetry. J Chromatogr A. 2003;993(1-2):29–37. https://doi.org/10.1016/S0021-9673(03)00392-3.
9. Togola A, Budzinski H. Analytical development for analysis of pharmaceuticals in water samples by SPE and GC-MS. Anal Bioanal Chem. 2007;388(3):627–635. https://doi.org/10.1007/s00216-007-1251-x.
10. Radjenović J, Petrović M, Barceló D. Analysis of pharmaceuticals in wastewater and removal using a membrane bioreactor. Anal Bioanal Chem. 2007;387(4):1365–1377. https://doi.org/10.1007/s00216-006-0883-6.
11. Jelić A, Gros M, Ginebreda A, Cespedes-Sánchez R, Ventura F, Petrovic M, Barcelo D. Occurrence, partition and removal of pharmaceuticals in sewage water and sludge during wastewater treatment. Water Res. 2011;45(3):1165–1176. https://doi.org/10.1016/j.watres.2010.11.010.
12. Falås P, Andersen HR, Ledin A, la Cour Jansen J. Occurrence and reduction of pharmaceuticals in the water phase at Swedish wastewater treatment plants. Water Sci Technol. 2012;66(4):783–791. https://doi.org/10.2166/wst.2012.243.
13. Jelić A, Petrović M, Barceló D. Multi-residue method for trace level determination of pharmaceuticals in solid samples using pressurised liquid extraction followed by liquid chromatography/quadrupole-linear ion trap mass spectrometry.Talanta. 2009;80:363–371. https://doi.org/10.1016/j.talanta.2009.06.077.
14. Sagristà E, Larsson E, Ezoddin M, Hidalgo M, Salvadó V, Jönsson JA. Determination of non-steroidal anti-inflammatory drugs in sewage sludge by direct hollow fiber supported liquid membrane extraction and liquid chromatography-mass spectrometry. J Chromatogr A. 2010;1217(40):6153–6158. https://doi.org/10.1016/j.chroma.2010.08.005.
15. Saleh A, Larsson E, Yamini Y, Jönsson JÅ. Hollow fiber liquid phase microextraction as a preconcentration and clean-up step after pressurized hot water extraction for the determination of non-steroidal anti-inflammatory drugs in sewage sludge. J Chromatogr A. 2011;1218(10):1331–1339. https://doi.org/10.1016/j.chroma.2011.01.011.
16. Al-Odaini NA, Zakaria MP, Yaziz MI, Surif S. Multi-residue analytical method for human pharmaceuticals and synthetic hormones in river water and sewage effluents by solid-phase extraction and liquid chromatography-tandem mass spectrometry. J Chromatogr A. 2010;1217(44):6791–6806. https://doi.org/10.1016/j.chroma.2010.08.033.
17. Christou A, Papadavid G, Dalias P, Fotopoulos V, Michael C, Bayona JM, Piña B, Fatta-Kassinos D. Ranking of crop plants according to their potential to uptake and accumulate contaminants of emerging concern. Environ Res. 2019;170:422–432. https://doi.org/10.1016/j.envres.2018.12.048.
18. Boxall AB, Johnson P, Smith EJ, Sinclair CJ, Stutt E, Levy LS. Uptake of veterinary medicines from soils into plants. J Agric Food Chem. 2006;54(6):2288–2297. https://doi.org/10.1021/jf053041t.
19. Herklotz PA, Gurung P, Vanden Heuvel B, Kinney CA. Uptake of human pharmaceuticals by plants grown under hydroponic conditions. Chemosphere. 2010;78(11):1416–1421. https://doi.org/10.1016/j.chemosphere.2009.12.048.

20. Bártíková H, Podlipná R, Skálová L. Veterinary drugs in the environment and their toxicity to plants. Chemosphere. 2016;144:2290–2301. https://doi.org/10.1016/j.chemosphere.2015.10.137.
21. Pan M, Chu LM. Fate of antibiotics in soil and their uptake by edible crops. Sci Total Environ. 2017;599/600:500–512. https://doi.org/10.1016/j.scitotenv.2017.04.214.
22. Tasho RP, Cho JY. Veterinary antibiotics in animal waste, its distribution in soil and uptake by plants: A review. Sci Total Environ. 2016;563/564:366–376. https://doi.org/10.1016/j.scitotenv.2016.04.140.
23. Wu X, Dodgen LK, Conkle JL, Gan J. Plant uptake of pharmaceutical and personal care products from recycled water and biosolids: a review. Sci Total Environ. 2015;536:655–666. https://doi.org/10.1016/j.scitotenv.2015.07.129. PMID:26254067.
24. Saloni J, Lipkowski P, Dasary SSR, Anjaneyulu Y, Yu H, Hill G. Theoretical study of molecular interactions of TNT, acrylic acid, and ethylene glycol dimethacrylate – Elements of molecularly imprinted polymer modeling process. Polymer (Guildf). 2011;52:1206–1216. https://doi.org/10.1016/j.polymer.2010.11.057.
25. Haginaka J, Sanbe H, Takehira H. Uniform-sized molecularly imprinted polymer for (S)-ibuprofen retention properties in aqueous mobile phases. J Chromatogr A. 1999;857(1-2):117–125. https://doi.org/10.1016/S0021-9673(99)00764-5. PMID:10536830.
26. Sun Z, Schüssler W, Sengl M, Niessner R, Knopp D. Selective trace analysis of diclofenac in surface and wastewater samples using solid-phase extraction with a new molecularly imprinted polymer. Anal Chim Acta. 2008;620(1-2):73–81. https://doi.org/10.1016/j.aca.2008.05.020.
27. Piletsky SA, Karim K, Piletska EV, Day CJ, Freebairn KW, Legge C, Turner APF. Recognition of ephedrine enantiomers by molecularly imprinted polymers designed using a computational approach. Analyst (Lond). 2001;126(10):1826–1830. https://doi.org/10.1039/b102426b.
28 Ellwanger A, Owens PK, Karlsson L, Bayoudh S, Cormack P, Sherrington D, Sellergren B. Application of molecularly imprinted polymers in supercritical fluid chromatography. J Chromatogr A. 2000;897(1-2):317–327. https://doi.org/10.1016/S0021-9673(00)00819-0.
29. Ansell RJ, Kuah JKL, Wang D, Jackson CE, Bartle KD, Clifford AA. Imprinted polymers for chiral resolution of (±)-ephedrine, 4: Packed column supercritical fluid chromatography using molecularly imprinted chiral stationary phases. J Chromatogr A. 2012;1264:117–123. https://doi.org/10.1016/j.chroma.2012.09.069.
30. Guo ZZ, Florea A, Cristea C, Bessueille F, Vocanson F, Goutaland F, Zhang AD, Săndulescu R, Lagarde F, Jaffrezic-Renault N. 1,3,5-Trinitrotoluene detection by a molecularly imprinted polymer sensor based on electropolymerisation of a microporous-metal-organic framework. Sens Actuators B Chem. 2015;207:960–966. https://doi.org/10.1016/j.snb.2014.06.137.
31. Prasad BB, Rai G. Molecular structure, vibrational spectra and quantum chemical MP2/DFT studies toward the rational design of hydroxyurea imprinted polymer. Spectrochim Acta A Mol Biomol Spectrosc. 2013;105:400–411. https://doi.org/10.1016/j.saa.2012.12.001.
32. Schwaiger J, Ferling H, Mallow U, Wintermayr H, Negele RD. Toxic effects of the non-steroidal anti-inflammatory drug diclofenac. Part I: histopathological alterations and bioaccumulation in rainbow trout. Aquat Toxicol. 2004;68(2):141–150. https://doi.org/10.1016/j.aquatox.2004.03.014.
33. Lin WC, Chen HC, Ding WH. Determination of pharmaceutical residues in waters by solid-phase extraction and large-volume on-line derivatization with gas chromatography-mass spectrometry. J Chromatogr A. 2005;1065(2):279–285. https://doi.org/10.1016/j.chroma.2004.12.081.
34. Baek IH, Han HS, Baik S, Helms V, Kim Y. Detection of acidic pharmaceutical compounds using virus-based molecularly imprinted polymers. Polymers (Basel). 2018;10(9):974–980. https://doi.org/10.3390/polym10090974.
35. Feng MX, Wang GN, Yang K, Liu HZ, Wang JP. Molecularly imprinted polymer-high performance liquid chromatography for the determination of tetracycline drugs in animal derived foods. Food Control. 2016;69:171–176. https://doi.org/10.1016/j.foodcont.2016.04.050.
36. Ji W, Xie H, Zhou J, Wang X, Ma X, Huang L. Water-compatible molecularly imprinted polymers for selective solid phase extraction of dencichine from the aqueous extract of Panax notoginseng. J Chromatogr B Analyt Technol Biomed Life Sci. 2016;1008:225–233. https://doi.org/10.1016/j.jchromb.2015.11.053.
37. Mamman S, Mohammad REA, Abdullahi SS, Birniwa AH, Chadi AS. Synthesis, characterisation and optimisation of magnetite molecularly imprinted polymer for application in the removal of nonsteroidal anti-inflammatory drugs (NSAIDS). ChemSearch J. 2020;11(1):1–8.
38. Madikizela LM, Chimuka L. Determination of ibuprofen, naproxen and diclofenac in aqueous samples using a multi-template molecularly imprinted polymer as selective adsorbent for solid-phase extraction. J Pharm Biomed Anal. 2016;128:210–215. https://doi.org/10.1016/j.jpba.2016.05.037.
39. Dai C, Zhang J, Zhang Y, Zhou X, Duan Y, Liu S. Selective removal of acidic pharmaceuticals from contaminated lake water using multi-templates molecularly imprinted polymer. Chem Eng J. 2012;211-212:302–309. https://doi.org/10.1016/j.cej.2012.09.090.
40. Madikizela LM, Chimuka L. Synthesis, adsorption and selectivity studies of a polymer imprinted with naproxen, ibuprofen and diclofenac. J Environ Chem Eng. 2016;4(4):4029–4037. https://doi.org/10.1016/j.jece.2016.09.012.
41. Navarro-Villoslada F, San Vicente B, Moreno-Bondi MC. Application of multivariate analysis to the screening of molecularly imprinted polymers for bisphenol A. Anal Chim Acta. 2004;504(1):149–162. https://doi.org/10.1016/S0003-2670(03)00766-9.
42. Tavengwa NT, Cukrowska E, Chimuka L. Synthesis, adsorption and selectivity studies of N-propyl quaternized magnetic poly(4-vinylpyridine) for hexavalent chromium. Talanta. 2013;116:670–677. https://doi.org/10.1016/j.talanta.2013.07.034.
43. Li Z, Qin C, Li D, Hou Y, Li S, Sun J. Molecularly imprinted polymer for specific extraction of hypericin from Hypericum perforatum L. herbal extract. J Pharm Biomed Anal. 2014;98:210–220. https://doi.org/10.1016/j.jpba.2014.05.031.
44. Manzo V, Ulisse K, Rodríguez I, Pereira E, Richter P. A molecularly imprinted polymer as the sorptive phase immobilized in a rotating disk extraction device for the determination of diclofenac and mefenamic acid in wastewater. Anal Chim Acta. 2015;889:130–137. https://doi.org/10.1016/j.aca.2015.07.038.
45. Ameli A, Alizadeh N. Nanostructured conducting molecularly imprinted polymer for selective uptake/release of naproxen by the electrochemically controlled sorbent. Anal Biochem. 2012;428(2):99–106. https://doi.org/10.1016/j.ab.2012.06.017.
46. Tang Y, Lan J, Gao X, Liu X, Zhang D, Wei L, Gao Z, Li J. Determination of clenbuterol in pork and potable water samples by molecularly imprinted polymer through the use of covalent imprinting method. Food Chem. 2016;190:952–959. https://doi.org/10.1016/j.foodchem.2015.06.067.
47. Bakhtiar S, Bhawani SA, Shafqat SR. Synthesis and characterisation of molecular imprinting polymer for removal of 2-phenylphenol from spiked blood serum and river water. Chem Biol Technol Agric. 2019;6(1):15. https://doi.org/10.1186/s40538-019-0152-5.
48. Sikiti P. Msagati TAM, Mamba BB, Mishra AK.Synthesis and characterisation of molecularly imprinted polymers for the remediation of PCBs and dioxins in aqueous environments. J Environ Health Sci Eng. 2014;12:82. https://doi.org/10.1186/2052-336X-12-82.
49. Guo P, Yuan X, Zhang J, Wang B, Sun X, Chen X, Zhao L. Dummy-surface molecularly imprinted polymers as a sorbent of micro-solid-phase extraction combined with dispersive liquid-liquid microextraction for determination of five 2-phenylpropionic acid NSAIDs in aquatic environmental samples. Anal Bioanal Chem. 2018;410(2):373–389. https://doi.org/10.1007/s00216-017-0727-6.
50. Skogsberg U, Meyer C, Rehbein J, Fischer G, Schauff S, Welsch N, Albert K, Hall AJ, Sellergren B. A solid-state and suspended-state magic angle spinning nuclear magnetic resonance spectroscopic investigation of a 9-ethyladenine molecularly imprinted polymer. Polymer (Guildf). 2007;48(1):229–238. https://doi.org/10.1016/j.polymer.2006.10.036.
51. Sobiech M, Żołek T, Luliński P, Maciejewska D. Separation of octopamine racemate on (R,S)-2-amino-1-phenylethanol imprinted polymer—experimental and computational studies. Talanta. 2016;146:556–567. https://doi.org/10.1016/j.talanta.2015.05.074.
52. Annanna KM, Beena M. Design of 2,4-dichlorophenoxyacetic acid imprinted polymer with high specificity and selectivity. Mater Sci Appl. 2011;2(3):131–140. https://doi.org/10.4236/msa.2011.23017.
53. Dai C, Zhang J, Zhang Y, Zhou X, Duan Y, Liu S. Selective removal of acidic pharmaceuticals from contaminated lake water using multi-templates

molecularly imprinted polymer. Chem Eng J. 2012;211-212:302–309. https://doi.org/10.1016/j.cej.2012.09.090.

54. Zunngu SS, Madikizela LM, Chimuka L, Mdluli PM. Synthesis and application of a molecularly imprinted polymer in the solid-phase extraction of ketoprofen from wastewater. C R Chim. 2017;20(5):585–591. https://doi.org/10.1016/j.crci.2016.09.006.
55. Santosda RC, Matheus S, Bruna NS, Laíse CP, Fabio AFD, César ACS, Keyller TT, Borgesa B. Assessment of surfactants on performance of molecularly imprinted polymer toward adsorption of pharmaceutical. J Environ Chem Eng. 2019;7(2):103037. https://doi.org/10.1016/j.jece.2019.103037.
56. Nimibofa A, Augustus NE, Donbebe W. Modelling and interpretation of adsorption isotherms. J Chem. 2017;303:11–13.
57. Chen Q, Tian Y, Li P, Yan C, Pang Y, Zheng L, Deng H, Zhou W, Meng X. Study on shale adsorption equation based on monolayer adsorption, multilayer adsorption, and capillary condensation. J Chem. 2017;2017:1496463. https://doi.org/10.1155/2017/1496463.